

# The Arctic Ocean in CMIP6 models: Biases and projected changes in temperature and salinity

Narges Khosravi<sup>1</sup>, Qiang Wang<sup>1,2</sup>, Nikolay Koldunov<sup>3,1</sup>, Claudia Hinrichs<sup>1</sup>,  
Tido Semmler<sup>1</sup>, Sergey Danilov<sup>1,4,5</sup>, Thomas Jung<sup>1,6</sup>

<sup>1</sup>Alfred Wegener Institute, Helmholtz Centre for Polar and Marine Research (AWI), Bremerhaven,  
Germany

<sup>2</sup>Laboratory for Regional Oceanography and Numerical Modeling, Pilot National Laboratory for Marine  
Science and Technology, Qingdao, China

<sup>3</sup>MARUM—Center for Marine Environmental Sciences, Bremen, Germany

<sup>4</sup>Department of Mathematics and Logistics, Jacobs University, Bremen, Germany

<sup>5</sup>A. M. Obukhov Institute of Atmospheric Physics Russian Academy of Science, Moscow, Russia

<sup>6</sup>Department of Physics and Electrical Engineering, University of Bremen, Bremen, Germany

## Key Points:

- A too deep and thick Arctic Atlantic Water layer continues to be a major issue in contemporary climate models contributing to the CMIP6
- The Arctic Ocean below the halocline is subject to much stronger warming than the global mean during the 21st century
- The upper ocean salinity is projected to decrease in the future by the multi-model mean. However, the uncertainty is considerable

---

Corresponding author: Narges Khosravi, [narges.khosravi@awi.de](mailto:narges.khosravi@awi.de)

Corresponding author: Qiang Wang, [Qiang.Wang@awi.de](mailto:Qiang.Wang@awi.de)

## Abstract

We examine the historical evolution and projected changes in the hydrography of the deep basin of the Arctic Ocean in 23 climate models participating in the Coupled Model Intercomparison Project Phase 6 (CMIP6). The comparison between historical simulations and an observational climatology shows that the simulated Atlantic Water (AW) layer is too deep and thick in the majority of models, including the multi-model mean (MMM). Moreover, the halocline is too fresh in the MMM. Overall our findings indicate that there is no obvious improvement in the representation of the Arctic hydrography in CMIP6 compared to CMIP5. The climate change projections reveal that the sub-Arctic seas are outstanding warming hotspots, causing a strong warming trend in the Arctic AW layer. The MMM temperature increase averaged over the upper 700 m at the end of the 21st century is about 40% and 60% higher in the Arctic Ocean than the global mean in the SSP245 and SSP585 scenarios, respectively. Salinity in the upper few hundred meters is projected to decrease in the Arctic deep basin in the MMM. However, the spread in projected salinity changes is rather large and the tendency toward stronger upper 400 m ocean stratification in the MMM is not simulated by all the models. The identified biases and projection uncertainties call for a concerted effort for major improvements of coupled climate models.

## Plain Language Summary

Coupled climate models are crucial tools for understanding and projecting climate change, especially for the Arctic where climate is changing at unprecedented rates. The Arctic Ocean has a strong halocline that separates warm Atlantic water in the mid-layer from the sea ice at the surface and so prevents melting from below. Weakening of the Arctic Ocean stratification might cause significant sea ice basal melting and accelerate sea ice decline. We examined the simulated temperature and salinity in the Arctic Ocean deep basin in state-of-the-art climate model simulations that provide the basis for the next IPCC Assessment Report. We find that the representation of Arctic temperature and salinity has not improved much in the new generation of climate models compared to previous versions. Moreover, we showed that the Arctic Ocean below the halocline is subject to a much stronger warming than the average global ocean. However, because of considerable spread in the ocean salinity projections the models do not agree on whether future changes in stratification will facilitate upward heat-fluxes from the Atlantic water layer to the base of sea ice or not. To increase the trustworthiness of projections, coupled climate models have to be improved substantially beyond the status quo.

## 1 Introduction

The Arctic is an integral part of the climate system that has undergone dramatic changes in recent decades. This includes the so-called Arctic amplification, which refers to atmospheric temperature increase in the Arctic that is at least two times higher than global mean values (Serreze & Francis, 2006), and that is associated with a rapid decrease in sea ice area and volume (Johannessen et al., 2004; Serreze & Stroeve, 2015; Notz & Stroeve, 2016; Dai et al., 2019). Like the atmosphere, the interior of the Arctic Ocean is also experiencing significant changes. Observations show an increase in the temperature of the Atlantic Water (AW) layer that occupies intermediate depths of the Arctic Ocean (Polyakov et al., 2005; Dmitrenko et al., 2008). Despite a strong freshening and thickening of the halocline in the western Arctic in recent decades (Giles et al., 2012; Q. Wang et al., 2016a; Proshutinsky et al., 2019), the isolation of the surface ocean and sea ice from warm AW has been found to have become weaker in the eastern Arctic (Polyakov et al., 2010; Ivanov et al., 2016); the latter process is commonly referred to as Arctic Atlantification (Polyakov et al., 2017).

69 To better understand these changes and provide trustworthy future projections,  
70 high-quality modelling of the Arctic Ocean, including the proper representation of crit-  
71 ical processes, such as water mass transformations and development of the Arctic At-  
72 lantification is required. This is especially important because of the limited amount of  
73 observational data from the Arctic, due to its remoteness, harsh environmental condi-  
74 tions, the presence of sea ice cover, and limited solar illumination that allow only restricted  
75 use of satellites to monitor ocean properties.

76 AW is the main oceanic heat source of the Arctic deep basin (Rudels & Friedrich,  
77 2000). The warm AW layer is characterized by high temperatures and salinity in com-  
78 parison to the halocline water, and potentially can impact the sea ice cover (Carmack  
79 et al., 2015; Dmitrenko et al., 2014; Polyakov et al., 2010). The AW inflow from the Nordic  
80 Seas consists of two branches: One through the Fram Strait by means of the West Spits-  
81 bergen Current, and the other one through the Barents Sea. Observations show that the  
82 Barents Sea branch loses most of its heat to the atmosphere already in the Barents Sea.  
83 This leaves the Fram Strait branch as the the major heat source of the Arctic AW layer  
84 (Smedsrud et al., 2013; Schauer et al., 2008). Part of the AW at the Fram Strait recir-  
85 culates southwards into the Greenland Sea (Marnela et al., 2013). In this context, it has  
86 been shown that the water mass properties at the Fram Strait as well as the partition  
87 of the West Spitsbergen Current into the Arctic interior can be significantly influenced  
88 by mesoscale eddies (Hattermann et al., 2016; Wekerle et al., 2017).

89 As the baroclinic Rossby radius in the Arctic Ocean is on the order of a few kilo-  
90 metres or less, even state-of-the-art ocean models used in climate simulations are too coarse  
91 to resolve mesoscale eddies. Although model developers tune their model parameteri-  
92 zations and parameters to improve the representation of the ocean circulation in the Arc-  
93 tic region, significant temperature and salinity biases still exist as shown in previous model  
94 intercomparison studies (Holloway et al., 2007; Proshutinsky & Kowalik, 2007; Proshutin-  
95 sky et al., 2016; Q. Wang et al., 2016a, 2016b; Ilıcak et al., 2016). In particular, both  
96 the ocean models analyzed in the Arctic Ocean Model Intercomparison Project (AOMIP)  
97 and the ocean components of global climate models analyzed in the Coordinated Ocean  
98 Ice Reference Experiments phase 2 (COREII) project show a large model spread in their  
99 simulated temperature and salinity in the Arctic halocline and AW layer when driven  
100 by atmospheric reanalysis forcing (Holloway et al., 2007; Ilıcak et al., 2016; Q. Wang et  
101 al., 2016a).

102 The Coupled Model Intercomparison Project (CMIP) was initiated by the World  
103 Climate Research Programme to provide a standardized framework for carrying out cli-  
104 mate change experiments with fully coupled models (Meehl et al., 2000). Although the  
105 fifth phase of CMIP (CMIP5) incorporated many of the same ocean models as those as-  
106 sessed in the COREII project (in ocean stand-alone simulations, (Ilıcak et al., 2016)),  
107 the model spread of Arctic Ocean temperature and salinity in CMIP5 models is signif-  
108 icantly larger than that in COREII models (Shu et al., 2019). The most probable ex-  
109 planation for this finding is that fully coupled models are further influenced by bias in  
110 atmospheric and land models as well as by biases that are amplified through two-way  
111 coupling between the ocean and the atmosphere. One major common issue in both forced  
112 ocean simulations and CMIP5 coupled model simulations is that the Arctic AW layer  
113 is too deep and too thick as reported in the aforementioned model assessment studies.

114 Currently, CMIP is in its sixth phase (CMIP6, Eyring et al., 2016) and it is cru-  
115 cial to analyse the performance of these models in simulating the present and the future  
116 state of temperature and salinity in the halocline and AW layer in the Arctic deep basin.  
117 Here, we examine the historical simulations and the future projections in CMIP6 cou-  
118 pled models. We focus on the following questions: (1) Can the available CMIP6 mod-  
119 els adequately reproduce the temperature and salinity in the Arctic deep basin? Specif-  
120 ically, we want to know whether the large temperature and salinity biases in the Arc-  
121 tic deep basin found in CMIP5 models are reduced in the CMIP6 models. (2) How will

122 the Arctic hydrography develop and how does the warming trend in the Arctic Ocean  
 123 deep basin compare to the global mean values in a warming world?

124 This paper is organized as follows: Data processing and methodology are described  
 125 in section 2. Subsequently, the results and discussion are presented in sections 3 and  
 126 4 respectively, followed by conclusions and suggestions for further investigations in sec-  
 127 tion 5.

## 128 2 Methodology and Data

129 We assess temperature and salinity in the CMIP6 historical simulations by com-  
 130 paring against the Polar Science Center Hydrographic Climatology (PHC) 3.0 database  
 131 (Steele et al., 2001). An alternative observational climatology is the temperature data  
 132 from the World Ocean Atlas 2018 (WOA18) (Locarnini et al., 2018) which as presented  
 133 in Figure 1a, is close to PHC3.0. However, we decided to use PHC3.0 as the main refer-  
 134 ence as WOA18 appears to be spatially discontinuous in temperature when plotted on  
 135 the same two-dimensional grid as the model data. The mean vertical distribution of tem-  
 136 perature and salinity in the Eurasian and Canadian basins are evaluated separately. These  
 137 are the deep ocean basins with bottom topography deeper than 300 m which are sep-  
 138 arated by the Lomonosov Ridge. For the sake of simplicity we will refer to the modelled  
 139 climatological mean as climatology hereafter which is calculated over 36 years (1979–2014)  
 140 of the historical experiments. Moreover, to assess possible future changes of the Arctic  
 141 Ocean, the climate change signals of the temperature and salinity are calculated by tak-  
 142 ing the difference between the present day and future values. Here we chose the defini-  
 143 tions for present day (1995–2014) and long-term future (2081–2100) conditions that are  
 144 consistent with those used in the upcoming IPCC AR6. Two Shared Socioeconomic Path-  
 145 ways (SSP) scenarios (O’Neill et al., 2016) are assessed in this study: SSP245 (the so-  
 146 called medium forcing scenario with  $4.5 \text{ W/m}^2$  forcing at the end of the century) and  
 147 SSP585 (the “high-end” of carbon emission or the strong forcing scenario with high car-  
 148 bon emission for radiative forcing of  $8.5 \text{ W/m}^2$  by 2100).

149 The CMIP6 model data is provided through the Earth System Grid Federation (ESGF).  
 150 The CMIP6 historical experiments cover the time period from 1850 to 2014. The pro-  
 151 jections from 2015 to 2100 are carried out as part of the scenario experiments, which de-  
 152 fine future scenarios based on approximate total radiative forcing levels by 2100. Among  
 153 the many models participating in CMIP6, so far only 23 models from 18 institutions (see  
 154 Table 1) have provided the required data from both their historical and SSP experiments.  
 155 Because there are different numbers of ensemble realizations available for different mod-  
 156 els and experiments, we only use the first ensemble member (r1i1p1f1) for each model  
 157 and experiment. A similar approach was used in a previous assessment of CMIP5 mod-  
 158 els (Shu et al., 2019).

159 The models have different grid resolutions and provide their three-dimensional data  
 160 (here sea-water potential temperature and salinity) on different depth levels. Before com-  
 161 puting the multi-model mean (MMM), all model outputs were re-gridded to the com-  
 162 mon grid for the PHC3.0 climatological data ( $1 \times 1^\circ$ ). Re-gridding was done using Cli-  
 163 mate Data Operators (CDO) (Schulzweida, 2019). Then, the re-gridded data were used  
 164 to produce the MMM fields. Likewise, when averaging over a vertical level was needed,  
 165 the individual model levels were interpolated to the 33 levels of the PHC3.0 data. How-  
 166 ever, given that individual models have different grid structures and topographies, re-  
 167 gridding them to the  $1 \times 1^\circ$  grid causes issues over continental slopes when calculating  
 168 the MMM (as indicated by grid scale noise). Nevertheless, none of the aspects mentioned  
 169 above is expected to impact the conclusions of this study.

170 For each model, the Atlantic Water Core Temperature (AWCT) is determined by  
 171 finding the maximum temperature along the vertical axis at each location. The depth

Table 1: The models for which data were made available (as of September 2020) on the Earth System Grid Federation server (<https://esgf-data.dkrz.de/projects/esgf-dkrz/>) for both historical and two selected scenario experiments (SSP245 and SSP585) of the following variables: potential temperature and salinity. KPP- k-profile parameterization by Large et al. (1994), TKE - Turbulent Kinetic Energy scheme based on the model of Gaspar et al. (1990), CTC - Turbulence closure scheme based on Canuto et al. (2001, 2002), EPBL - Energetically constrained parameterization of the surface boundary layer (Reichl & Hallberg, 2018), PP - Richardson number-dependent scheme of Pacanowski and Philander (1981), NK - surface mixed layer parameterization of Noh and Jin Kim (1999). GLS - generic length scale scheme of Umlauf and Burchard (2003).

No.	Model Name	Institution ID	Grid Resolution (lon × lat)	Number of levels	Mixing scheme
1	ACCESS-CM2	CSIRO-ARCCSS	360 × 300	50	KPP
2	ACCESS-ESM1-5	CSIRO-ARCCSS	360 × 300	50	KPP
3	AWI-CM-1-1-MR	AWI	Unstructured grid ca. 25 km res	46	KPP
4	BCC-CSM2-MR	BCC	360 × 232	40	KPP
5	CAMS-CSM1-0	CAMS	360 × 200	50	KPP
6	CanESM5	CCCma	360 × 291	45	TKE
7	CESM2	NCAR	320 × 384	60	KPP
8	CESM2-WACCM	NCAR	320 × 384	60	KPP
9	CIESM	THU	384 × 320	60	KPP
10	CMCC-CM2-SR5	CMCC	363 × 292	50	TKE
11	EC-Earth3	EC-Earth-Consortium	362 × 292	75	TKE
12	EC-Earth3-Veg	EC-Earth-Consortium	362 × 292	75	TKE
13	FGOALS-g3	CAS	360 × 218	30	CTC
14	GFDL-CM4	NOAA-GFDL	1440 × 1080	35	EPBL
15	GFDL-ESM4	NOAA-GFDL	720 × 576	35	EPBL
16	INM-CM4-8	INM	360 × 180	33	PP
17	INM-CM5-0	INM	360 × 180	33	PP
18	IPSL-CM6A-LR	IPSL	363 × 332	75	TKE
19	MIROC6	MIROC	360 × 256	63	NK
20	MPI-ESM1-2-HR	MPI-M	802 × 404	40	PP
21	MPI-ESM1-2-HR	MPI-M	256 × 220	40	PP
22	MRI-ESM2-0	MRI	360 × 363	61	GLS
23	NESM3	NUIST	362 × 292	46	TKE

172 at which the maximum temperature occurs is defined as the Atlantic Water Core Depth  
173 (AWCD). In order to eliminate outlier results and for the outcome to be comparable to  
174 the assessment of CMIP5 AW layer, we implemented the same criterion as Shu et al. (2019)  
175 when calculating MMM. That is, if the simulated AWCD in any of the two basins is deeper  
176 than four times that of the observation, then the model is not considered in the MMM  
177 calculation (see Figure 2).

### 178 3 Results

#### 179 3.1 Model evaluation from historical simulations

180 The vertical profiles of observed hydrography highlight the vertical structure of the  
181 Arctic Ocean water mass in the Eurasian and Canadian basins (Figure 1). Averaged over

182 each basin, the halocline is located above about 200m and 300m in the Eurasian and Cana-  
 183 dian basins, respectively. Below the cold halocline the warm AW layer can be found, which  
 184 occupies the layer between the halocline and about 800 m depth (as indicated by the depth  
 185 of the 0°C). According to the observational data, the mean AWCT is about 1° and 0.5°C  
 186 and the mean AWCD amounts to about 300m and 500m in the Eurasian and Canadian  
 187 basins, respectively. Although the MMM reproduces the main vertical structure of the  
 188 temperature and salinity to some extent, there are substantial biases. More specifically,  
 189 the simulated MMM AWCD is about 250m deeper than observed; and the simulated AW  
 190 layer is too thick with its lower boundary reaching to a depth of about 3000m, instead  
 191 of about 800m in the observation (Figure 1a). This is very similar to the results of CMIP5  
 192 models (Shu et al., 2019).

193 Inspection of individual models reveals that most of the models overestimate the  
 194 AWCD (Figure 2a). There are three models with AWCD similar to or smaller than the  
 195 observations in either basin; however, their AWCT is much lower than observed (Fig-  
 196 ure 2b). In particular, four models have extremely deep AW in at least one of the basins  
 197 (depicted with white color in Figure 2a); hence they are excluded when calculating the  
 198 MMM as described in Section 2. Even with these models excluded, the model spread (de-  
 199 fined by the standard deviation; std) of the AWCD is as large as about 250m in both  
 200 basins (Figure 2a). The model spread of the AWCT is also quite pronounced in both basins  
 201 (about 1°C, Figure 2b). Note, that the range (difference between the maximum and the  
 202 minimum) of AWCT in the models is more than 3.5°C in both basins. It is also worth  
 203 noting, that the biases for AWCD and AWCT are very similar in the two basins for all  
 204 models, which may not be too surprising given that the Canadian basin lies “downstream”  
 205 of the Eurasian one (see below).

206 The spatial patterns of the MMM AWCT and AWCD are compared to observa-  
 207 tional estimates in Figure 3. The observations clearly show the AW pathway: AW en-  
 208 ters the Arctic Ocean through the Fram Strait and circulates cyclonically along the con-  
 209 tinental slope in the Eurasian Basin; it then penetrates into the Canadian Basin in a cy-  
 210 clonic direction. The AWCD deepens along the AW pathway, and it is on average about  
 211 200m deeper in the Canadian Basin than in the Eurasian Basin (see also Figure 1a and  
 212 Figure 2a). The MMM AWCT is colder than observed nearly everywhere inside the Arc-  
 213 tic Ocean, although its spatial pattern indicates that, on average, the simulated AW cir-  
 214 culation is cyclonic as expected. The MMM AWCD reproduces the contrast between the  
 215 two deep basins (deeper in the Canadian Basin); however, AWCD is overestimated by  
 216 models in both basins. There are differences in the detailed spatial pattern of AWCD  
 217 between the MMM and the observation. One outstanding difference is that the observed  
 218 maximum is in the southeastern Canadian Basin, whereas in the MMM it is located in  
 219 the western Canadian Basin.

220 The simulated salinity also has large biases in both basins, which are most pronounced  
 221 in the halocline and at the surface (Figure 1b). The MMM salinity has negative biases  
 222 up to 0.5 psu in the halocline in the Canadian Basin, and even larger biases in the Eurasian  
 223 Basin. The largest fresh bias is closer to the surface in the Eurasian basin than in the  
 224 Canadian Basin given that the halocline is thinner in the Eurasian Basin. At the sur-  
 225 face, the MMM salinity bias is negative in the Eurasian Basin and slightly positive in  
 226 the Canadian Basin. Inspecting individual models reveals that the models have a large  
 227 spread in the simulated salinity in the upper 400 m. The largest spread is at the surface,  
 228 with the difference between the maximum and minimum surface salinity reaching more  
 229 than 5 psu. Even at 200 m depth, the range of the simulated salinity between the mod-  
 230 els is still more than 1 psu. Although the MMM underestimates the upper ocean (~ 400  
 231 m) salinity on average (thus overestimating the Arctic freshwater content), some mod-  
 232 els do significantly overestimate the upper ocean salinity.

233 Upper ocean salinity in model simulations can be significantly influenced by ver-  
 234 tical mixing coefficients (Zhang & Steele, 2007), so different vertical mixing parameter-

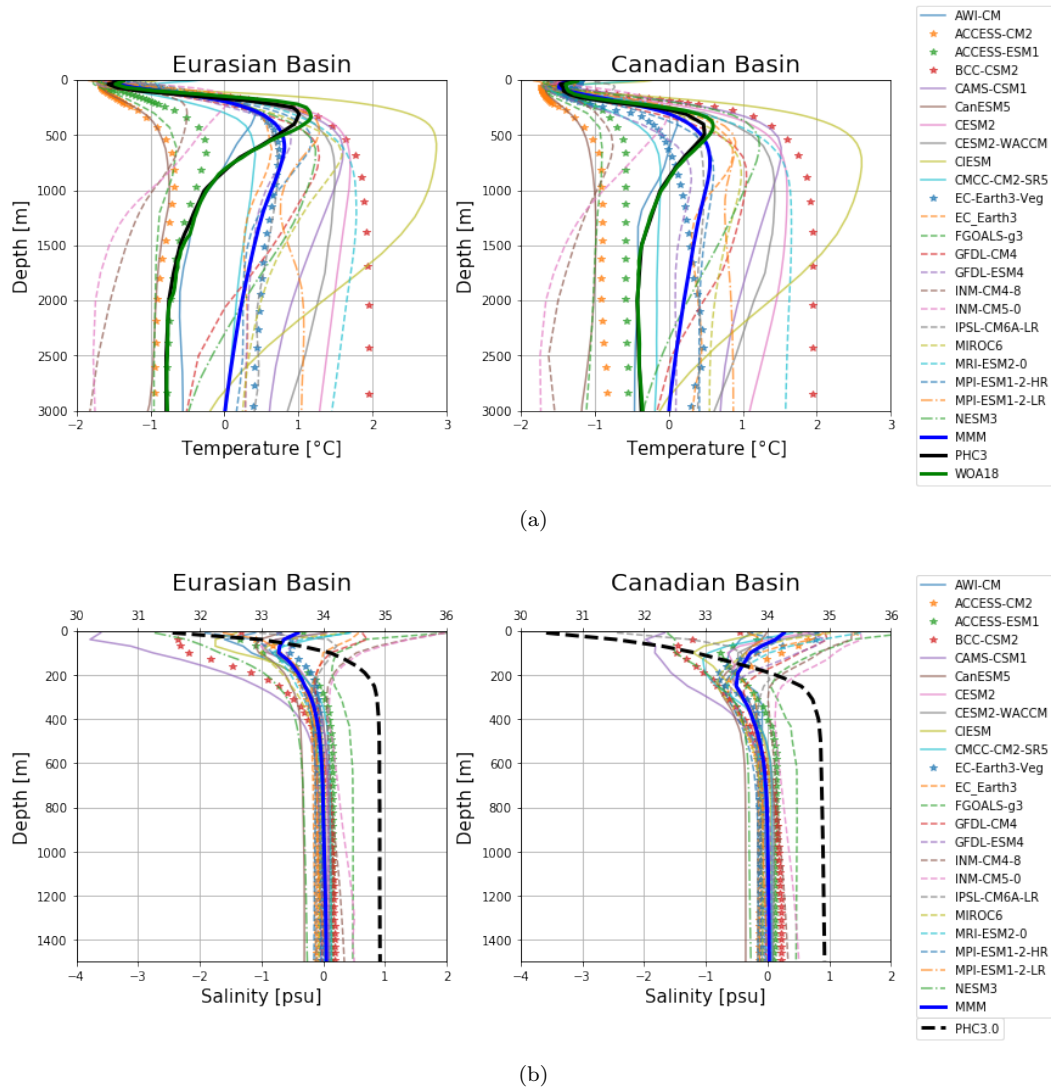


Figure 1: Climatological (1979–2014) and basin mean potential temperature (top) and salinity bias (bottom) profile in the Arctic Ocean. The Eurasian basin is shown on the left and Canadian basin in the right panels. The 19 models, which are taken into account for generating the multi-model means (MMM), are shown as thin solid and dashed lines. The four models excluded from the MMM are marked differently (with stars). For temperature profiles the thick blue, black and green curves represent the MMM and the PHC3.0 and WOA18 climatologies, respectively. Note that in contrast to temperature, salinity profiles are presented as *biases* with respect to the PHC3.0 climatology; The black dashed curve represents the PHC3.0 observation itself (not the bias) with the corresponding salinity values shown on the upper x-axis. The thick blue curve is the MMM bias. The original salinity profiles are shown in Figure S1.

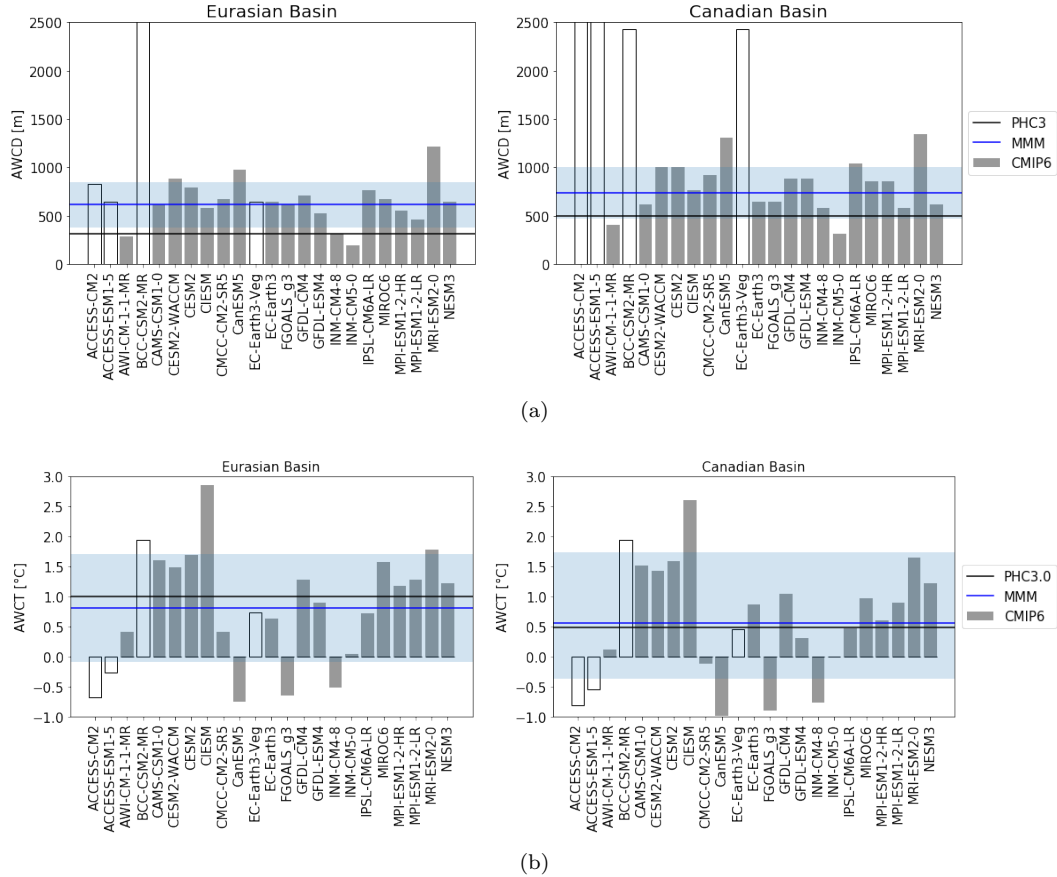


Figure 2: Atlantic Water core depth (AWCD, in m) and Atlantic Water core temperature (AWCT, in °C) from the individual CMIP6 models (bars), multi-model-mean (blue solid line) and PHC3.0 climatology (black solid line) for the Eurasian and Canadian basins. White bars represent models that have been discarded from further analysis (i.e. models with AWCD larger than 4 times that of the observation). The models shown with white bars are excluded in the multi-model mean. The multi-model mean  $\pm$  one standard deviation range is indicated through light blue shading.

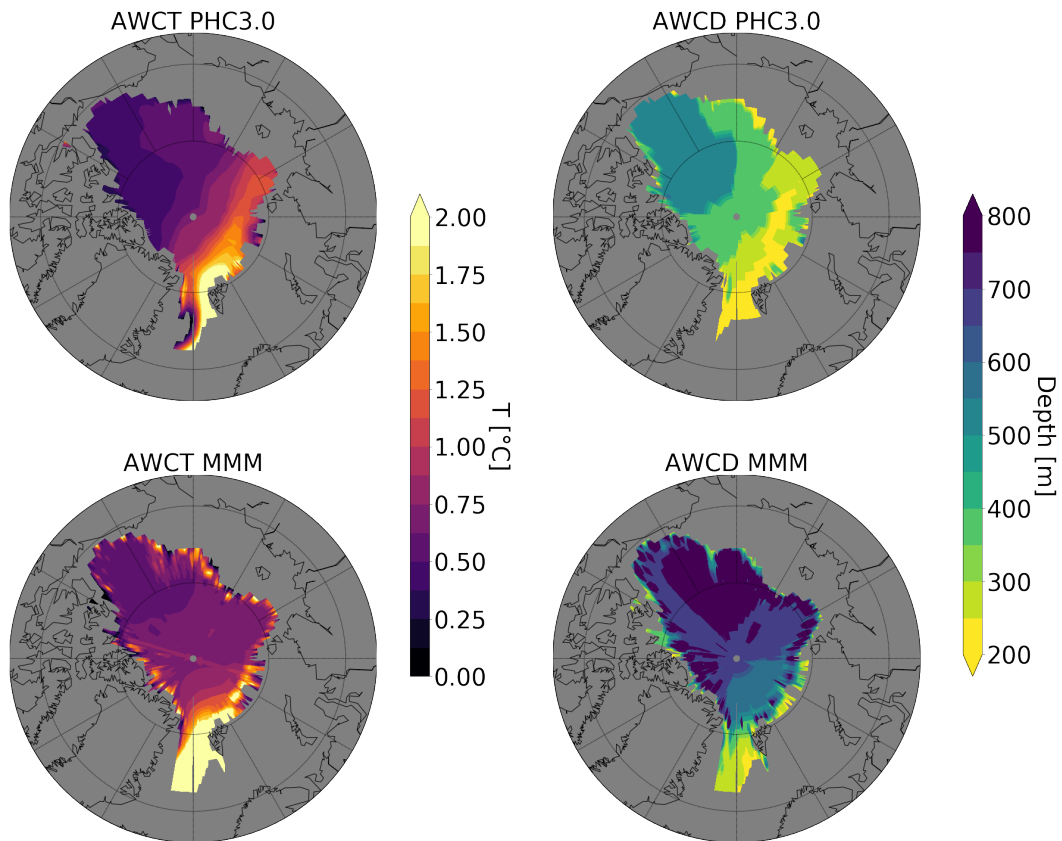


Figure 3: The climatological mean Atlantic water core temperature (AWCT in °C) and Atlantic water core depth (AWCD in m) from PHC3.0 (upper panels) and the MMM of 19 CMIP6 models (historical experiment; 1979–2014, lower panels).

235 izations and different levels of numerical vertical mixing between the models can explain  
 236 part of the model spread in salinity. Among other factors, Arctic freshwater sources, in-  
 237 cluding river runoff and precipitation, which typically have considerable spread in cli-  
 238 mate model simulations (Shu et al., 2018), can also contribute to the identified model  
 239 spread in upper ocean salinity. The largest MMM salinity bias is in the mid to lower halo-  
 240 cline, so on average it is probably more related to vertical mixing in the ocean.

241 In summary, CMIP6 historical simulations show a too deep and too thick AW layer  
 242 and a too fresh halocline in a MMM sense, and they show considerable model spread in  
 243 the simulated temperature and salinity. These issues are the same as in CMIP5 mod-  
 244 els (Shu et al., 2019). Importantly, not only can these “high-level” issues be found in CMIP5  
 245 and CMIP6 models; also some details, such as the location of maximum AWCD (Fig-  
 246 ure 3) and opposite biases in MMM sea surface salinity between the two basins (Figure  
 247 1b), are essentially the same in the two generations of CMIP models. Therefore, for the  
 248 representation of the Arctic hydrography, CMIP6 does not show clear improvements com-  
 249 pared to CMIP5.

### 250 3.2 Climate change projections

251 In this section, we will explore the climate change signals of Arctic temperature  
 252 and salinity for two scenarios (i.e. ssp245 and ssp585). Climate change for zonal mean  
 253 temperature in the Arctic deep basins as simulated by CMIP6 models is presented in Fig-  
 254 ure 4. In both scenarios, ocean warming mainly occurs in the upper 2000 m. This holds  
 255 for MMM as well as most individual models. For both basins and scenarios the strongest  
 256 warming signal for MMM is found in two depth ranges – that is at depths close to the  
 257 observed AWCD (about 200–500 m depth) and at the surface. The former indicates the  
 258 warming of the AW layer, while the latter reflects the surface warming associated with  
 259 sea ice decline, Arctic Amplification and increasing ocean heat inflow from the Pacific.  
 260 In both scenarios, the warming in the AW layer is stronger in the Eurasian Basin than  
 261 in the Canadian Basin. This is consistent with the fact that the AW circulates cycloni-  
 262 cally from the Eurasian Basin to the Canadian Basin. For MMM the maximum climate  
 263 change signal for the AW temperature amounts to about 1.7°C (1.4°C) in the Eurasian  
 264 (Canadian) Basin in SSP245, while it is about 3°C and 2.4°C in the two basins in SSP585,  
 265 respectively. At the surface, the climate change signals in the two basins are compar-  
 266 able. In fact, the MMM surface temperature climate change amounts to about 1° and 2.8°  
 267 in the SSP245 and SSP585 scenarios, respectively. Only in the Canadian Basin and for  
 268 the more extreme SSP585 scenario is projected climate change in surface temperature  
 269 larger than that in the AW layer (by up to about 0.4°C). As the strongest warming in  
 270 the AW layer is at depth shallower than the simulated AWCD in historical simulations  
 271 (cf. Figure 1b and Figure 4), the AWCD becomes shallower at the end of the 21st cen-  
 272 tury (by about 200 m in both warming scenarios, see Figure. S2).

273 The spatial patterns of MMM climate change signals for AWCT are consistent with  
 274 the source region and circulation direction of AW (Figure 5). In both scenarios the strongest  
 275 warming signal starts at the Fram Strait, the entrance of the warm AW; it then prop-  
 276 agates into and around the Eurasian Basin and then Canadian Basin. The warming at  
 277 the Fram Strait amounts to more than 2°C and 4°C in the SSP245 and SSP585 scenar-  
 278 ios, respectively. The warming signal does not propagate from the Eurasian Basin to the  
 279 Canadian Basin in a strictly cyclonic direction along the boundary of the deep basins  
 280 (anticipated from existing knowledge of the Arctic ocean circulation), as indicated by  
 281 the extension of the warming signal from the Eurasian Basin toward the Canadian Basin  
 282 through the central Arctic. As the model resolutions in CMIP6 models are typically quite  
 283 coarse, the associated numerical diffusion is most probably the main reason for such a  
 284 spatially diffused pattern of anthropogenic warming in the central Arctic ocean.

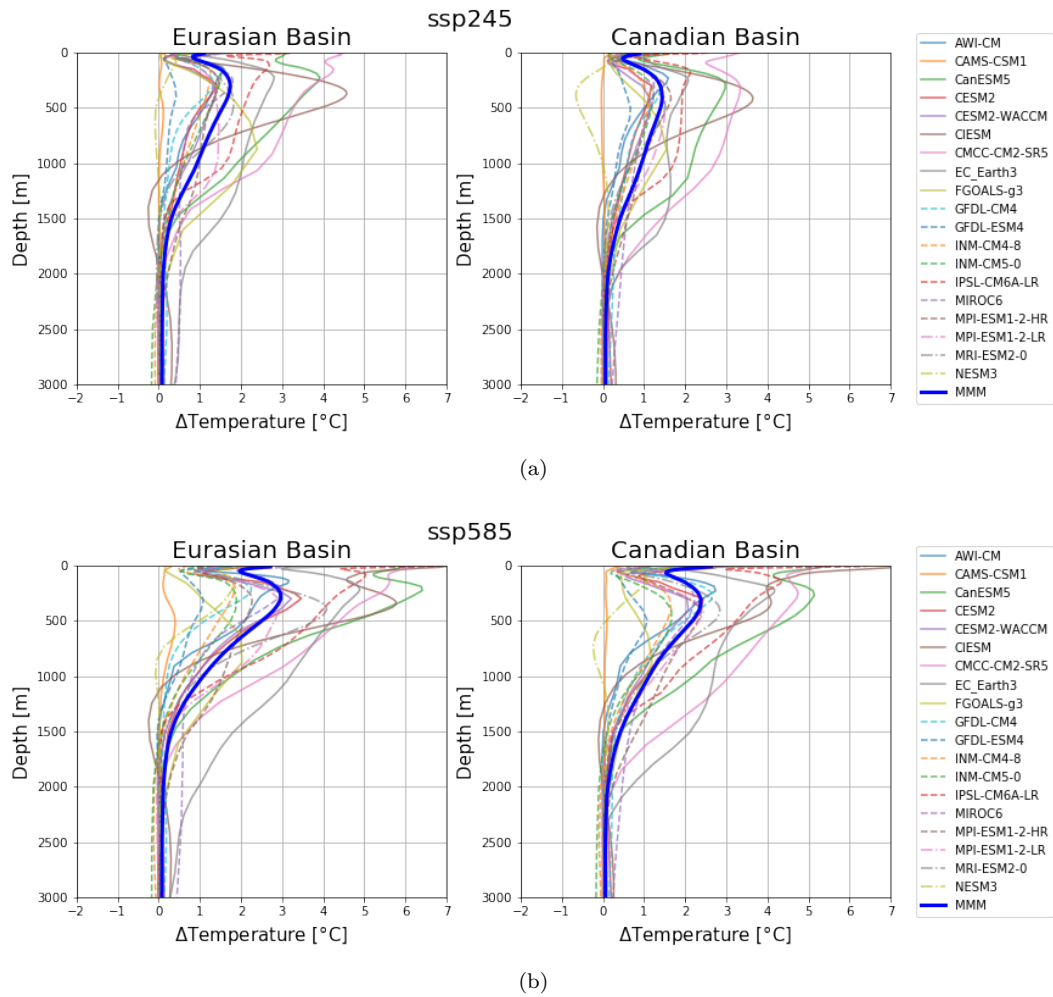


Figure 4: Projected climate change in potential temperature for the Eurasian (left) and Canadian (right) basins based on two CMIP6 scenarios: SSP245 (top) and SSP585 (bottom). Climate change is defined as the difference between the periods 2081-2100 and 1995-2014.

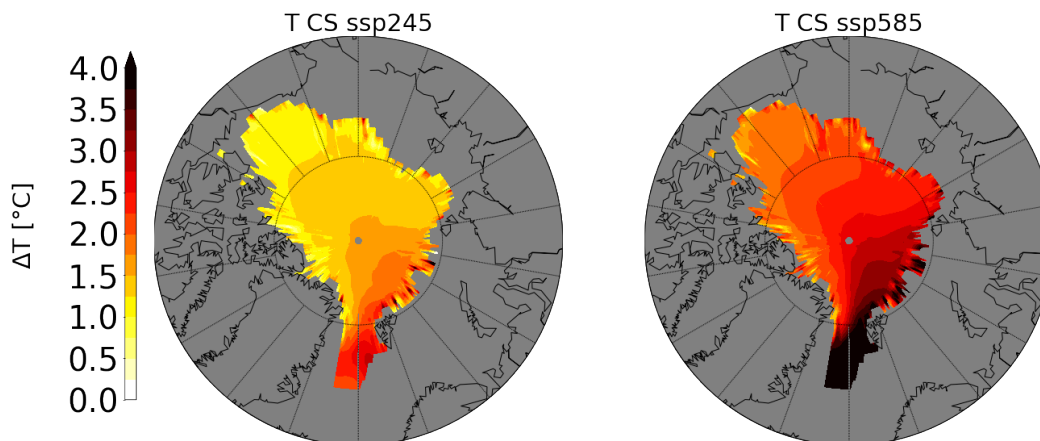


Figure 5: Projected climate change of the Atlantic Water core temperature (AWCT) for the Arctic deep basin generated using two CMIP6 scenarios: SSP245 (left) and SSP585 (right). Climate change is defined as the difference between the periods 2081-2100 and 1995-2014.

285 Despite the large warming trend in the MMM, the individual models show a large  
 286 spread of the climate change signals for temperature. Not all of these signals from in-  
 287 dividual models are physically consistent with those of the MMM (Figure 4, for model  
 288 spread see also the Hovmöller diagrams of temperature for individual models in Figure  
 289 S3). The range of the climate change signals of temperature among the models is about  
 290 4°C in SSP245 and 7°C in SSP585; this is more than twice that of the MMM climate change  
 291 signals. There are even two models with negligible or even negative temperature changes  
 292 in the core depth range of the AW layer in both scenarios, while all other models pre-  
 293 dict ocean warming in the AW layer. Furthermore, the models do not agree on whether  
 294 the ocean surface or the AW layer will warm more in the future. In both basins and in  
 295 both scenarios, there are models with relatively stronger warming at the surface and mod-  
 296 els with stronger warming in the AW layer.

297 To compare the extent of projected warming in the Arctic deep basin with the pro-  
 298 jected global mean warming, Hovmöller diagrams for MMM temperature for these two  
 299 ocean areas are shown in Figure 6a. In the Arctic Ocean, the strongest warming trend  
 300 can be seen at the depth where AW prevails, while the surface ocean shows a compar-  
 301 atively smaller warming trend, as can be seen in Figure 4. In contrast, the maximum global  
 302 average warming trend is at the ocean surface. Although the global mean surface warm-  
 303 ing trend is stronger than the mean over the Arctic surface, the warming in the AW layer  
 304 of the Arctic Ocean causes stronger overall warming in the Arctic deep basin, as indi-  
 305 cated by the time series of mean temperature averaged over the upper 700 m and upper  
 306 2000 m (Figure 6b). The increase in temperature averaged over the upper 700 m of  
 307 the Arctic deep basin at the end of the 21 century is higher than that of the global ocean  
 308 by 0.4° (40%) and 1° (60%) in the SSP245 and SSP585 scenarios, respectively. Although  
 309 the amplitude of the temperature increase averaged over the upper 2000 m is smaller than  
 310 averaged over the upper 700 m, the amplified warming in the Arctic deep basin is even  
 311 more pronounced. It is about 75% higher in the Arctic deep basin than in the global deep  
 312 basin at the end of the 21st century in the SSP585 scenario. It is worth stressing that  
 313 the warming in the Arctic Ocean has just started to be significant from the 2020s ac-  
 314 cording to the MMM; in contrast the temperature change is rather small from the be-  
 315 ginning of the industrialization to the present day (see the Hovmöller diagram for Ar-  
 316 ctic temperature covering the whole CMIP historical simulation period in Figure S4).

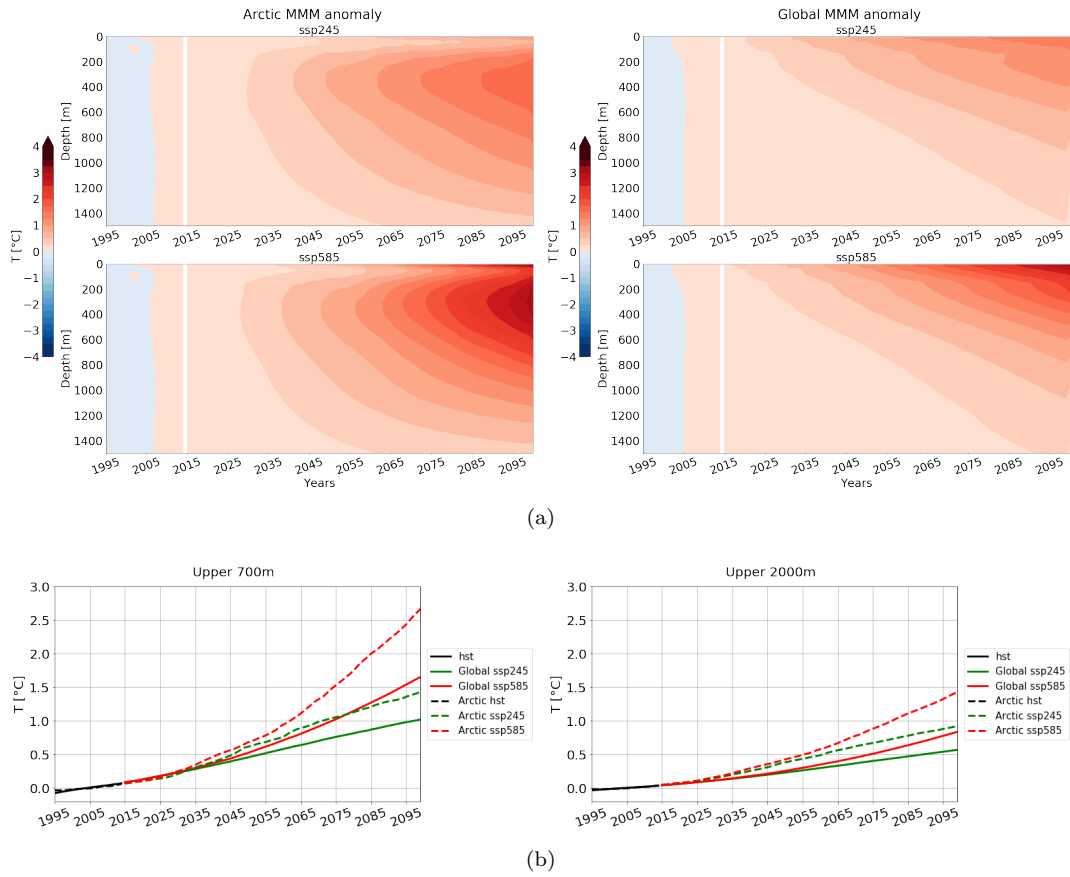


Figure 6: (a) Hovmöller diagrams of temperature anomalies (depth vs. time) for the Arctic Ocean (left) and global ocean (right). Only ocean areas with bottom bathymetry deeper than 300 m are considered. (b) Time series of temperature anomalies averaged over the upper 700 m (left) and 2000 m (right). Temperature anomalies are relative to the average over the present day (1995–2014) period.

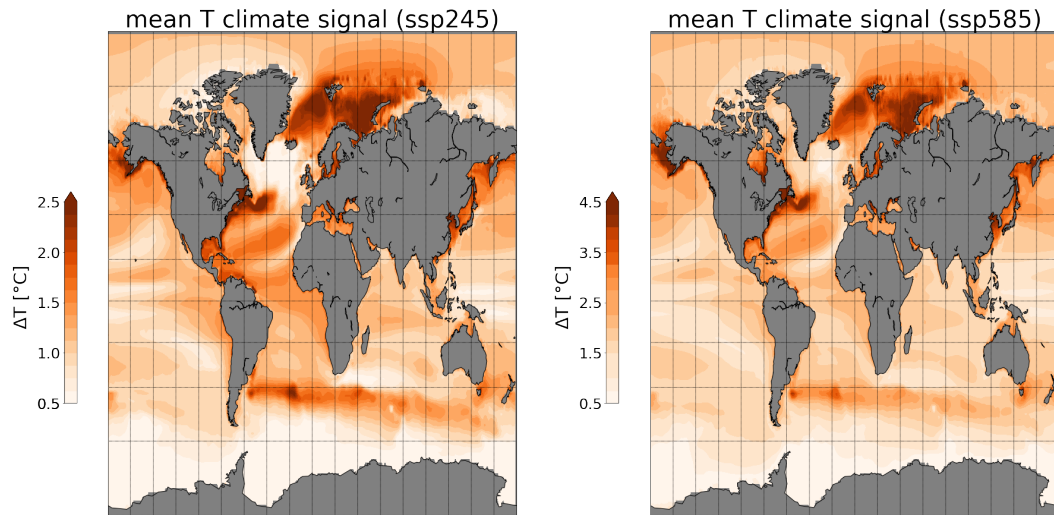


Figure 7: Projected temperature change averaged over upper 700 m in the SSP245 (left) and SSP585 (right) scenarios. Climate change is defined as the difference between the periods 2081–2100 and 1995–2014

317 The strong warming trend in the Arctic Ocean is consistent with the intense warming  
 318 in the inflow waters (Figure 7). The projected climate change for the temperature  
 319 averaged over the upper 700 m reveals that the sub-Arctic seas close to the Arctic Ocean  
 320 inflow gateways are all warming hotspots, namely the northern Nordic Sea, the Barents  
 321 Sea and the Bering Sea. The warming in these hotspots is stronger than most of the world  
 322 ocean areas. The warming in the Pacific Water inflow, which mainly enters the upper  
 323 Arctic Ocean, could partially explain the enhanced surface warming in the Canadian Basin,  
 324 especially in the ssp585 scenario (Figure 4). The significant warming of the Arctic AW  
 325 layer (Figure 5) can be associated with the warming of the AW entering the deep basins.  
 326 The CMIP6 projections indicate that the currently observed ocean warming associated  
 327 with Arctic Pacification and Arctic Atlantification (Timmermans et al., 2018; Polyakov  
 328 et al., 2017, 2020) will continue to develop in future warming climate.

329 For the climate change signals of salinity, in both basins there is a freshening of the  
 330 upper 400 m ocean in both scenarios (Figure 8). The strongest freshening occurs in the  
 331 upper halocline and in the mixed layer (upper 200 m), indicating an increase in fresh-  
 332 water storage in the Arctic Ocean in the future. The freshening is consistent with an en-  
 333 hanced hydrological cycle, and thus increased freshwater supply to the Arctic Ocean in  
 334 a warming climate (Carmack et al., 2015; Shu et al., 2018). The freshening is stronger  
 335 in the Canadian Basin than in the Eurasian Basin, quite possibly due to changes in the  
 336 ocean surface stress induced by sea ice decline (Q. Wang et al., 2019; Q. Wang, 2021;  
 337 S. Wang et al., 2021). On average the surface Ekman transport is directed from the Eurasian  
 338 Basin toward the Canadian Basin. Sea ice decline increases ocean surface stress, thus  
 339 the Ekman transport, which enhances freshwater accumulation in the Canadian Basin  
 340 and tends to reduce it in the Eurasian Basin (Q. Wang et al., 2019).

341 Although salinity for MMM shows freshening in the Arctic Ocean in both warm-  
 342 ing scenarios, some of the models predict an increase of salinity in the upper 200 m depth,  
 343 either near the surface or in the halocline (Figure 8). The range of projected salinity changes  
 344 among the models amounts to about 2-3 psu even when the “outlier models” are excluded,  
 345 which is much larger than the MMM salinity climate change signal. The large model spread  
 346 in the simulated salinity in the future scenarios implies large spread in the simulated fu-

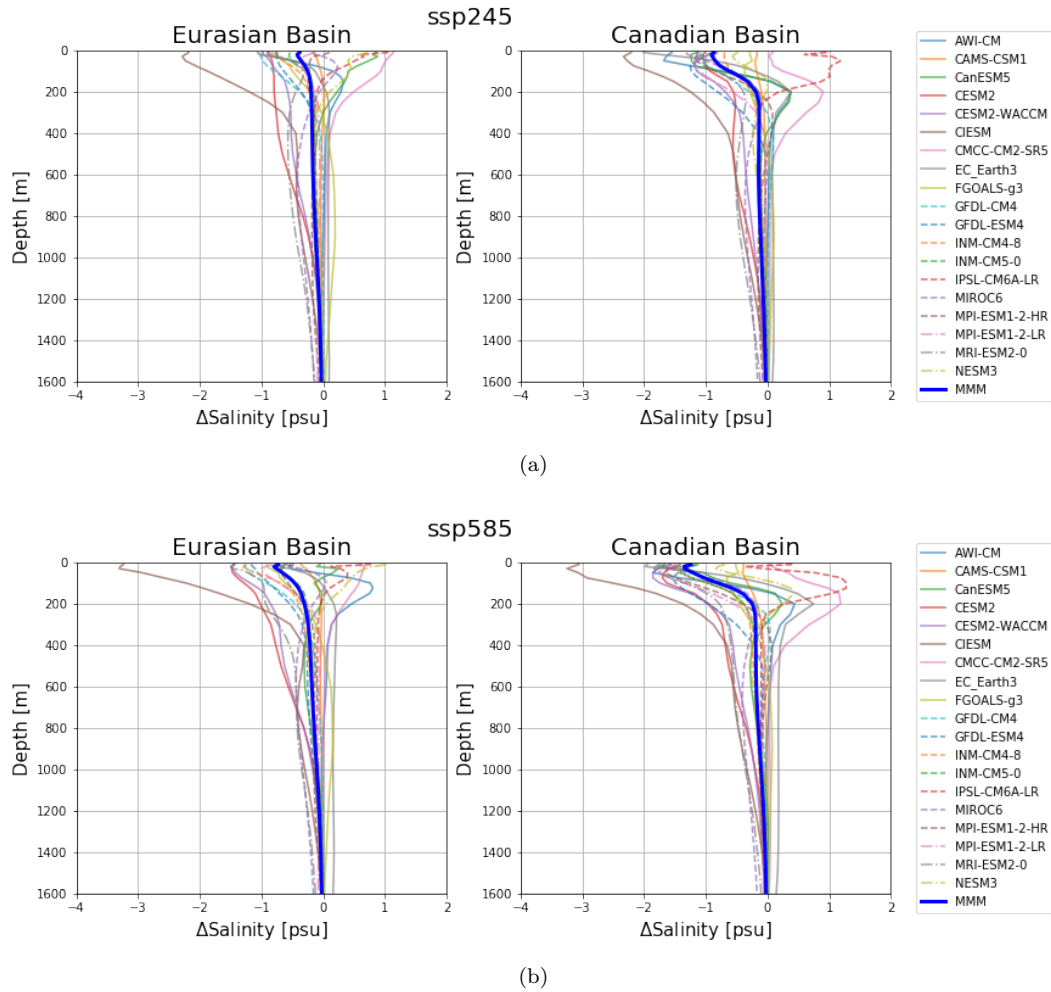


Figure 8: The salinity climate change signals for Eurasian and Canadian basins in CMIP6 projections ssp245 (top) and ssp585 (bottom). The climate change signal is defined as the difference between two periods (2081–2100 minus 1995–2014) according to IPCC AR6.

347 future Arctic freshwater storage in CMIP6 models. Therefore, the issue of large spread in  
 348 Arctic freshwater storage simulated in CMIP5 models (Shu et al., 2018) remains nearly  
 349 unchanged in CMIP6 models.

350 In summary, the CMIP6 MMM shows strong warming in the Arctic AW layer and  
 351 at the surface for both future scenarios considered in this study. The AW layer is likely  
 352 to become shallower. The warming in the bulk of the AW layer may cause the temper-  
 353 ature climate change in the Arctic deep basins to be much larger than the global mean  
 354 change at depth. The Arctic halocline is likely to become much fresher in the future, in  
 355 particular in the Canadian Basin. However, the CMIP6 models have large spread and  
 356 thus uncertainty in the simulated climate change signals for both temperature and salin-  
 357 ity.

## 4 Discussion

Most of the state-of-the-art CMIP6 models simulate a warm AW layer below the cold halocline in the Arctic Ocean, which is one of the key characteristics of the Arctic Ocean evident from observations. However, the simulated AW layer is too thick and too deep compared to observations in most of the models and also in the MMM. This issue has been found in forced ocean simulations more than a decade ago (Holloway et al., 2007); it was prevalent in both forced and coupled ocean simulations in the period of CMIP5 (Ilıcak et al., 2016; Shu et al., 2019), and it continues to remain a critical issue in CMIP6 models, as shown by our analysis. There is agreement across the above-mentioned studies that numerical mixing in coarse resolution models is a main reason for this issue. Indeed, it was found that increasing horizontal resolution to 4.5 km in the Arctic Ocean, although not fully eddy resolving yet, can significantly reduce the too thick and too deep biases of the AW layer (Q. Wang et al., 2018). The CMIP6 models tend to have a too fresh mid to lower halocline (with MMM salinity biases of more than 0.5 psu), as in CMIP5 models (Shu et al., 2019), which means a weaker stratification in the associated depth range. Strong diapycnal mixing can weaken the halocline stratification (Zhang & Steele, 2007). So it seems likely that the diapycnal numerical mixing associated with coarse model resolution is partially responsible for the salinity bias too.

We did not find clear correlation relationship between model performance and model horizontal resolution in the analyzed CMIP6 models. The reason could be that the horizontal resolutions in CMIP6 models are still coarse (Table 1), and much coarser than the resolution of 4.5 km that was found to be very effective in reducing long-standing model biases in ocean-only configurations (Q. Wang et al., 2018). Even in the HighResMIP of CMIP6, the spatial resolution in the Arctic Ocean does not exceed 1/4 degree (Docquier et al., 2019). Nevertheless, these models can improve the AW heat transport toward the Arctic Ocean to some extent in comparison to the models using 1 degree resolution — thus encouraging the use of higher model resolution in future CMIP efforts, as suggested by Docquier et al. (2019). There is ongoing effort to reduce numerical mixing through improving model formulations (Griffies et al., 2020). As the model biases discussed above are likely to be associated with numerical mixing in the models, it remains to be seen whether such improvement can lead to breakthroughs in model performance in the Arctic Ocean in next generations of CMIP simulations.

The MMM shows that the upper ocean including the upper halocline and mixed layer will become fresher in a warming climate (Figure 8), while, simultaneously, the AW layer will become warmer and the AWCD will become shallower (Figure 4 and Figure S2). The uplift and warming of the AW layer implies that winter convection, if it happens, does not need to reach very deep to bring up ocean heat. This will be especially true in the Eurasian Basin, because the decrease in upper ocean salinity, thus the increase in stratification, is much smaller in the Eurasian Basin than in the Canadian Basin in the MMM (Figure 8). However, the models have large spread in the projected salinity and temperature changes in both scenarios. Some models show salinification in the upper ocean, thus weakening in the ocean stratification, while some models indicate upper ocean freshening that is much stronger than the MMM, thus a significant increase in the ocean stratification (Figure 8). Therefore, the models do not agree on changes in the strength of vertical mixing and the possibility of emergence of deep convection in the Arctic deep basin as well. In order to predict the future development of the Arctic Atlantification and its possible impact on sea ice, model uncertainties need to be considerably reduced. As some of the model biases identified in this paper could have origins outside the Arctic Ocean and possibly in other components of the climate system, major efforts to systematically reduce model uncertainties in the future CMIP simulations are required.

## 5 Conclusion

In this study, we assessed the temperature and salinity in the Arctic deep basin (the Eurasian and Canadian basins) in CMIP6 historical simulations and the respective climate change projections (SSP245 and SSP585 scenarios). One of our main findings is that the biases in Arctic Ocean temperature and salinity found in CMIP5 historical simulations remain virtually unchanged in the CMIP6 simulations. The Atlantic Water (AW) layer is still too deep and too thick in nearly all models, the multi-model-mean (MMM) halocline is too fresh, and the models have a large spread in both the simulated temperature and salinity. Even some details in model biases in CMIP6 models are similar to those in CMIP5 models. Therefore, it can be concluded that there is essentially no improvement in the representation of the hydrography in the Arctic deep basins from CMIP5 to CMIP6.

Both the Arctic AW layer and upper 700 m ocean are projected to become warmer in the future as indicated by the CMIP6 MMM. The warming in the Arctic deep basins in the future (2081–2100) relative to the present day conditions (1995–2014) is largest in the upper AW layer (200–500 m) for MMM, with a magnitude of about 1.7°C (3°C) and 1.4°C (2.4°C) in the Eurasian and Canadian basins in SSP245 (SSP585). The warming results in an uplift of the AW layer. The corresponding climate change signal of ocean surface temperature amounts to about 1°C and 2.8°C in the SSP245 and SSP585 scenarios, respectively. Furthermore, it is shown that in the depth range of the Arctic AW layer, the Arctic Ocean has a stronger warming trend than the global mean. Averaged over the upper 700 m, the increase in Arctic basin temperature at the end of the 21st century is 40% and 60% higher than the global mean in the SSP245 and SSP585 scenarios, respectively. The warming in the Arctic Ocean is even stronger than that in most of the world ocean basins on average. We further found that all the sub-Arctic seas close to the Arctic inflow gateways are warming hotspots in a warming climate, including the northern Nordic Seas, Barents Sea and eastern Bering Sea. In particular, the strong warming in the AW inflow supplies the warming of the Arctic AW layer. The warming trend in the AW inflow is not only induced by warming upstream in the North Atlantic, but also can be enhanced by local atmospheric warming around the Arctic gateways (Shu et al., 2021; Asbjørnsen et al., 2020) and feedback processes (Q. Wang et al., 2020).

The MMM upper 400 m ocean salinity is found to decrease in both Arctic basins in the future scenarios, with the decrease in the Canadian Basin being stronger than in the Eurasian Basin. Therefore, the stratification in the Arctic upper ocean is projected to be more stable in the MMM in both the SSP245 and SSP585 scenarios. However, the models show a large spread in the simulated climate change for upper ocean salinity, with some models indicating upper ocean salinification and some freshening. The upper ocean stratification influences the strength of vertical mixing, and thus potentially the impact of AW layer on sea ice. Therefore, CMIP6 models do not agree on the extent to which the future changes in AW layer may influence the sea ice. The identified model biases in CMIP6 models reported in this study call for a concerted effort to improve climate coupled models in support of future CMIP beyond incremental.

## Acknowledgments

The work described in this paper has received funding from the European Union's Horizon 2020 Research Innovation programme through grant agreement No. 727862 APPLICATE. The content of the paper is the sole responsibility of the authors and it does not represent the opinion of the European Commission, and the Commission is not responsible for any use that might be made of the information contained. This work is also supported by the German Helmholtz Climate Initiative REKLIM (Regional Climate Change). This paper is a contribution to the projects S1 (Diagnosis and Metrics in Climate Models) and S2 (Improved parameterizations and numerics in climate models) of the Collaborative Research Centre TRR 181 "Energy Transfer in Atmosphere and Ocean" funded

461 by the Deutsche Forschungsgemeinschaft (DFG, German Research Foundation) – project  
 462 no. 274762653. The CMIP6 data were downloaded from [https://esgf-data.dkrz.de/  
 463 projects/esgf-dkrz/](https://esgf-data.dkrz.de/projects/esgf-dkrz/) and PHC3 data from [http://psc.apl.washington.edu/nonwp  
 464 \\_projects/PHC/Data3.html](http://psc.apl.washington.edu/nonwp_projects/PHC/Data3.html)

## 465 References

- 466 Asbjørnsen, H., Årthun, M., Skagseth, Ø., & Eldevik, T. (2020). Mechanisms un-  
 467 derlying recent arctic atlantification. *Geophysical Research Letters*, *47*(15),  
 468 e2020GL088036.
- 469 Canuto, V., Howard, A., Cheng, Y., & Dubovikov, M. (2001). Ocean turbulence.  
 470 part i: One-point closure model—momentum and heat vertical diffusivities.  
 471 *Journal of Physical Oceanography*, *31*(6), 1413–1426.
- 472 Canuto, V., Howard, A., Cheng, Y., & Dubovikov, M. (2002). Ocean turbu-  
 473 lence. part ii: Vertical diffusivities of momentum, heat, salt, mass, and passive  
 474 scalars. *Journal of Physical Oceanography*, *32*(1), 240–264.
- 475 Carmack, E., Polyakov, I., Padman, L., Fer, I., Hunke, E., Hutchings, J., . . . others  
 476 (2015). Toward quantifying the increasing role of oceanic heat in sea ice loss  
 477 in the new arctic. *Bulletin of the American Meteorological Society*, *96*(12),  
 478 2079–2105.
- 479 Dai, A., Luo, D., Song, M., & Liu, J. (2019). Arctic amplification is caused by sea-  
 480 ice loss under increasing co<sub>2</sub>. *Nature communications*, *10*(1), 121.
- 481 Dmitrenko, I. A., Kirillov, S. A., Serra, N., Koldunov, N., Ivanov, V. V., Schauer,  
 482 U., . . . others (2014). Heat loss from the atlantic water layer in the northern  
 483 kara sea: Causes and consequences. *Ocean Science*, *10*(4), 719–730.
- 484 Dmitrenko, I. A., Polyakov, I. V., Kirillov, S. A., Timokhov, L. A., Frolov, I. E.,  
 485 Sokolov, V. T., . . . Walsh, D. (2008). Toward a warmer arctic ocean: Spread-  
 486 ing of the early 21st century atlantic water warm anomaly along the eurasian  
 487 basin margins. *Journal of Geophysical Research: Oceans*, *113*(C5).
- 488 Docquier, D., Grist, J. P., Roberts, M. J., Roberts, C. D., Semmler, T., Ponsoni,  
 489 L., . . . others (2019). Impact of model resolution on arctic sea ice and north  
 490 atlantic ocean heat transport. *Climate Dynamics*, *53*(7-8), 4989–5017.
- 491 Eyring, V., Bony, S., Meehl, G. A., Senior, C. A., Stevens, B., Stouffer, R. J., &  
 492 Taylor, K. E. (2016). Overview of the coupled model intercomparison project  
 493 phase 6 (cmip6) experimental design and organization. *Geoscientific Model  
 494 Development (Online)*, *9*(LLNL-JRNL-736881).
- 495 Gaspar, P., Grégoris, Y., & Lefevre, J.-M. (1990). A simple eddy kinetic energy  
 496 model for simulations of the oceanic vertical mixing: Tests at station papa and  
 497 long-term upper ocean study site. *Journal of Geophysical Research: Oceans*,  
 498 *95*(C9), 16179–16193.
- 499 Giles, K. A., Laxon, S. W., Ridout, A. L., Wingham, D. J., & Bacon, S. (2012).  
 500 Western arctic ocean freshwater storage increased by wind-driven spin-up of  
 501 the beaufort gyre. *Nature Geoscience*, *5*(3), 194–197.
- 502 Griffies, S. M., Adcroft, A., & Hallberg, R. W. (2020). A primer on the vertical  
 503 lagrangian-remap method in ocean models based on finite volume generalized  
 504 vertical coordinates. *Journal of Advances in Modeling Earth Systems*, *12*(10),  
 505 e2019MS001954.
- 506 Hattermann, T., Isachsen, P. E., von Appen, W.-J., Albrechtsen, J., & Sundfjord, A.  
 507 (2016). Eddy-driven recirculation of atlantic water in fram strait. *Geophysical  
 508 Research Letters*, *43*(7), 3406–3414.
- 509 Holloway, G., Dupont, F., Golubeva, E., Häkkinen, S., Hunke, E., Jin, M., . . . others  
 510 (2007). Water properties and circulation in arctic ocean models. *Journal of  
 511 Geophysical Research: Oceans*, *112*(C4).
- 512 Ilıcak, M., Drange, H., Wang, Q., Gerdes, R., Aksenov, Y., Bailey, D., . . . others  
 513 (2016). An assessment of the arctic ocean in a suite of interannual core-ii

- 514 simulations. part iii: Hydrography and fluxes. *Ocean Modelling*, *100*, 141–161.
- 515 Ivanov, V., Alexeev, V., Koldunov, N. V., Repina, I., Sandø, A. B., Smedsrud, L. H.,  
516 & Smirnov, A. (2016). Arctic ocean heat impact on regional ice decay: A sug-  
517 gested positive feedback. *Journal of Physical Oceanography*, *46*(5), 1437–1456.
- 518 Johannessen, O. M., Bengtsson, L., Miles, M. W., Kuzmina, S. I., Semenov, V. A.,  
519 Alekseev, G. V., . . . others (2004). Arctic climate change: observed and mod-  
520 elled temperature and sea-ice variability. *Tellus A: Dynamic meteorology and*  
521 *oceanography*, *56*(4), 328–341.
- 522 Large, W. G., McWilliams, J. C., & Doney, S. C. (1994). Oceanic vertical mixing: A  
523 review and a model with a nonlocal boundary layer parameterization. *Reviews*  
524 *of Geophysics*, *32*(4), 363–403.
- 525 Locarnini, M., Mishonov, A., Baranova, O., Boyer, T., Zweng, M., Garcia, H., . . .  
526 others (2018). World ocean atlas 2018, volume 1: Temperature.
- 527 Marnela, M., Rudels, B., Houssais, M.-N., Beszczynska-Möller, A., Eriksson, P., et  
528 al. (2013). Recirculation in the fram strait and transports of water in and  
529 north of the fram strait derived from ctd data. *Ocean Science*.
- 530 Meehl, G. A., Boer, G. J., Covey, C., Latif, M., & Stouffer, R. J. (2000). The cou-  
531 pled model intercomparison project (cmip). *Bulletin of the American Meteorolo-*  
532 *gical Society*, *81*(2), 313–318.
- 533 Noh, Y., & Jin Kim, H. (1999). Simulations of temperature and turbulence structure  
534 of the oceanic boundary layer with the improved near-surface process. *Journal*  
535 *of Geophysical Research: Oceans*, *104*(C7), 15621–15634.
- 536 Notz, D., & Stroeve, J. (2016). Observed arctic sea-ice loss directly follows anthro-  
537 pogenic co2 emission. *Science*, *354*(6313), 747–750.
- 538 O'Neill, B. C., Tebaldi, C., Vuuren, D. P. v., Eyring, V., Friedlingstein, P., Hurtt,  
539 G., . . . others (2016). The scenario model intercomparison project (scenari-  
540 omip) for cmip6. *Geoscientific Model Development*, *9*(9), 3461–3482.
- 541 Pacanowski, R., & Philander, S. (1981). Parameterization of vertical mixing in nu-  
542 merical models of tropical oceans. *Journal of Physical Oceanography*, *11*(11),  
543 1443–1451.
- 544 Polyakov, I. V., Alkire, M. B., Bluhm, B. A., Brown, K. A., Carmack, E. C.,  
545 Chierici, M., . . . others (2020). Borealization of the arctic ocean in response  
546 to anomalous advection from sub-arctic seas. *Frontiers in Marine Science*, *7*,  
547 491.
- 548 Polyakov, I. V., Beszczynska, A., Carmack, E. C., Dmitrenko, I. A., Fahrbach, E.,  
549 Frolov, I. E., . . . others (2005). One more step toward a warmer arctic. *Geo-*  
550 *physical Research Letters*, *32*(17).
- 551 Polyakov, I. V., Pnyushkov, A. V., Alkire, M. B., Ashik, I. M., Baumann, T. M.,  
552 Carmack, E. C., . . . others (2017). Greater role for atlantic inflows on sea-ice  
553 loss in the eurAsian basin of the arctic ocean. *Science*, *356*(6335), 285–291.
- 554 Polyakov, I. V., Timokhov, L. A., Alexeev, V. A., Bacon, S., Dmitrenko, I. A.,  
555 Fortier, L., . . . others (2010). Arctic ocean warming contributes to reduced  
556 polar ice cap. *Journal of Physical Oceanography*, *40*(12), 2743–2756.
- 557 Proshutinsky, A., & Kowalik, Z. (2007). Preface to special section on arctic ocean  
558 model intercomparison project (aomip) studies and results. *Journal of Geo-*  
559 *physical Research: Oceans*, *112*(C4).
- 560 Proshutinsky, A., Krishfield, R., Toole, J., Timmermans, M.-L., Williams, W., Zim-  
561 mermann, S., . . . others (2019). Analysis of the beaufort gyre freshwater  
562 content in 2003–2018. *Journal of Geophysical Research: Oceans*, *124*(12),  
563 9658–9689.
- 564 Proshutinsky, A., Steele, M., & Timmermans, M.-L. (2016). Forum for arctic mod-  
565 eling and observational synthesis (famos): Past, current, and future activities.  
566 *Journal of Geophysical Research: Oceans*, *121*(6), 3803–3819.
- 567 Reichl, B. G., & Hallberg, R. (2018). A simplified energetics based planetary bound-  
568 ary layer (epbl) approach for ocean climate simulations. *Ocean Modelling*, *132*,

- 569 112–129.
- 570 Rudels, B., & Friedrich, H. J. (2000). The transformations of atlantic water in the  
571 arctic ocean and their significance for the freshwater budget. In *The freshwater*  
572 *budget of the arctic ocean* (pp. 503–532). Springer.
- 573 Schauer, U., Beszczynska-Möller, A., Walczowski, W., Fahrbach, E., Piechura, J.,  
574 & Hansen, E. (2008). Variation of measured heat flow through the fram  
575 strait between 1997 and 2006. In *Arctic–subarctic ocean fluxes* (pp. 65–85).  
576 Springer.
- 577 Schulzweida, U. (2019). *Cdo user guide (version 1.9. 6)*.
- 578 Serreze, M. C., & Francis, J. A. (2006). The arctic amplification debate. *Climatic*  
579 *change*, 76(3-4), 241–264.
- 580 Serreze, M. C., & Stroeve, J. (2015). Arctic sea ice trends, variability and impli-  
581 cations for seasonal ice forecasting. *Philosophical Transactions of the Royal*  
582 *Society A: Mathematical, Physical and Engineering Sciences*, 373(2045),  
583 20140159.
- 584 Shu, Q., Qiao, F., Song, Z., Zhao, J., & Li, X. (2018). Projected freshening of the  
585 arctic ocean in the 21st century. *Journal of Geophysical Research: Oceans*,  
586 123(12), 9232–9244.
- 587 Shu, Q., Wang, Q., Song, Z., & Qiao, F. (2021). The poleward enhanced arctic  
588 ocean cooling machine in a warming climate. *Nature communications*, 12(1),  
589 1–9.
- 590 Shu, Q., Wang, Q., Su, J., Li, X., & Qiao, F. (2019). Assessment of the atlantic  
591 water layer in the arctic ocean in cmip5 climate models. *Climate Dynamics*,  
592 53(9-10), 5279–5291.
- 593 Smedsrud, L. H., Esau, I., Ingvaldsen, R. B., Eldevik, T., Haugan, P. M., Li, C., ...  
594 others (2013). The role of the barents sea in the arctic climate system. *Reviews*  
595 *of Geophysics*, 51(3), 415–449.
- 596 Steele, M., Morley, R., & Ermold, W. (2001). Phc: A global ocean hydrography with  
597 a high-quality arctic ocean. *Journal of Climate*, 14(9), 2079–2087.
- 598 Timmermans, M.-L., Toole, J., & Krishfield, R. (2018). Warming of the interior arc-  
599 tic ocean linked to sea ice losses at the basin margins. *Science advances*, 4(8),  
600 eaat6773.
- 601 Umlauf, L., & Burchard, H. (2003). A generic length-scale equation for geophysical  
602 turbulence models. *Journal of Marine Research*, 61(2), 235–265.
- 603 Wang, Q. (2021). Stronger variability in the arctic ocean induced by sea ice de-  
604 cline in a warming climate: Freshwater storage, dynamic sea level and surface  
605 circulation. *Journal of Geophysical Research: Oceans*, 126(3), e2020JC016886.
- 606 Wang, Q., Ilicak, M., Gerdes, R., Drange, H., Aksenov, Y., Bailey, D. A., ... others  
607 (2016a). An assessment of the arctic ocean in a suite of interannual core-ii  
608 simulations. part ii: Liquid freshwater. *Ocean Modelling*, 99, 86–109.
- 609 Wang, Q., Ilicak, M., Gerdes, R., Drange, H., Aksenov, Y., Bailey, D. A., ... others  
610 (2016b). An assessment of the arctic ocean in a suite of interannual core-ii sim-  
611 ulations. part i: Sea ice and solid freshwater. *Ocean Modelling*, 99, 110–132.
- 612 Wang, Q., Wekerle, C., Danilov, S., Sidorenko, D., Koldunov, N., Sein, D., ... Jung,  
613 T. (2019). Recent sea ice decline did not significantly increase the total liquid  
614 freshwater content of the arctic ocean. *Journal of Climate*, 32(1), 15–32.
- 615 Wang, Q., Wekerle, C., Danilov, S., Wang, X., & Jung, T. (2018). A 4.5 km resolu-  
616 tion arctic ocean simulation with the global multi-resolution model fesom1. 4.  
617 *Geosci. Model Dev.*, 11, 1229–1255.
- 618 Wang, Q., Wekerle, C., Wang, X., Danilov, S., Koldunov, N., Sein, D., ... Jung, T.  
619 (2020). Intensification of the atlantic water supply to the arctic ocean through  
620 fram strait induced by arctic sea ice decline. *Geophysical Research Letters*,  
621 47(3), e2019GL086682.
- 622 Wang, S., Wang, Q., Shu, Q., Song, Z., Lohmann, G., Danilov, S., & Qiao, F.  
623 (2021). Nonmonotonic change of the arctic ocean freshwater storage capability

- 624 in a warming climate. *Geophysical Research Letters*, *48*(10), e2020GL090951.  
625 Wekerle, C., Wang, Q., von Appen, W.-J., Danilov, S., Schourup-Kristensen, V., &  
626 Jung, T. (2017). Eddy-resolving simulation of the atlantic water circulation  
627 in the fram strait with focus on the seasonal cycle. *Journal of Geophysical*  
628 *Research: Oceans*, *122*(11), 8385–8405.
- 629 Zhang, J., & Steele, M. (2007). Effect of vertical mixing on the atlantic water  
630 layer circulation in the arctic ocean. *Journal of geophysical research: Oceans*,  
631 *112*(C4).